ORGANOMETALLICS

Article

pubs.acs.org/Organometallics

Anticancer Ruthenium(η^6-*p*-cymene) Complexes of Nonsteroidal Anti-inflammatory Drug Derivatives

Farhana Aman,[†,‡] Muhammad Hanif,[†,§] Waseeq Ahmad Siddiqui,*[,‡] Adnan Ashraf,[†,‡] Lukas K. Filak,[†] Jóhannes Reynisson,[†] Tilo Söhnel,[†] Stephen M. F. Jamieson,[∥] and Christian G. Hartinger*[,†]

[†]School of Chemical Sciences, University of Auckland, Private Bag 92019, Auckland 1142, New Zealand

[‡]Department of Chemistry, University of Sargodha, Sargodha 40100, Pakistan

[§]Department of Chemistry, COMSATS Institute of Information Technology, Abbottabad 22060, Pakistan

[∥]Auckland Cancer Society Research Centre, University of Auckland, Private Bag 92019, Auckland 1142, New Zealand

Supporting Information

ABSTRACT: Oxicams are a versatile family of heterocyclic compounds, and the two representatives meloxicam and piroxicam are widely used drugs for the treatment of a variety of inflammatory and rheumatic diseases in humans. As cancer-associated inflammation is known to occur in carcinogenesis, we aimed to combine compounds carrying bioactive oxicam moieties with ruthenium(arene) fragments, known for anticancer activity. Ru^{II}(arene) complexes with methyl ester derivatives of the oxicam scaffold were prepared and characterized by standard methods and crystallographically.

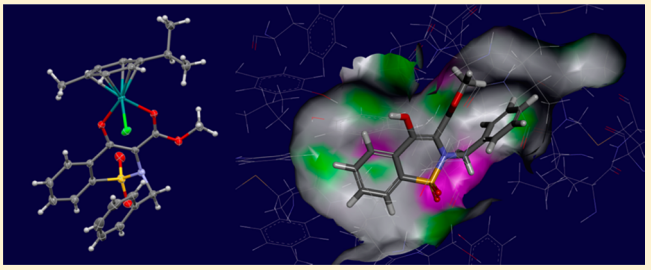

The organoruthenium compounds formed from $Ru^{II}(\eta^6$-*p*-cymene) chlorido moieties and oxicam-based ligands were subjected to bioanalytical investigations to establish their physicochemical properties with regard to stability in DMSO and water as well as reactivity toward the amino acids L-histidine (His), L-methionine (Met), and L-cysteine (Cys) and the DNA model compound guanosine 5′-monophosphate (5′-GMP). The compounds hydrolyzed rapidly in water to give the respective aqua complexes, formed amino acid complexes with Met and His, but decompose with Cys, while interaction with 5′-GMP was through its phosphate residue. The anticancer activity of the complexes against the colon carcinoma HCT116 and breast cancer MDA MB 231 cancer cell lines was established using an *in vitro* assay. The cytotoxicity was found strongly dependent on the lipophilicity of the compound, as was shown through correlation with log k_w and clog *P* values of the ligands. The most lipophilic compound [chlorido(methyl 4-oxido-2-benzyl-2*H*-1,2-benzothiazine-3-carboxylate-1,1-dioxide)(η^6-*p*-cymene)ruthenium(II)] was the most active in the cell assays, with an IC_{50} of 80 μM in HCT116 cells.

Metallochemotherapeutics and in particular platinum-based complexes are well-established treatment options for a wide array of neoplastic diseases. The anticancer activity of platinum drugs is attributed to their ability to bind DNA.[1] Their remarkable success has been marred somewhat due to intrinsic and acquired resistance of tumors and adverse side effects.[2]

With the aim to improve efficacy and reduce undesirable side effects, a large number of complexes of platinum and other metals were tested for their tumor-inhibiting properties. Out of those, ruthenium complexes emerged as a promising class of anticancer agents,[3] and two Ru(III) complexes are currently in phase II clinical trials. NAMI-A (imidazolium *trans*-[tetrachlorido(dimethyl sulfoxide)(1*H*-imidazole)ruthenate-(III)]) inhibits metastasis, whereas KP1019 (indazolium *trans*-[tetrachloridobis(1*H*-indazole)ruthenate(III)]) and also its more water-soluble analogue KP1339 (sodium *trans*-[tetrachloridobis(1*H*-indazole)ruthenate(III)]) showed potent activity in a number of primary human tumor models.[4,5]

In recent years a half-sandwich-configured organoruthenium-(arene) scaffold emerged as a versatile tool for the design of novel anticancer agents, often with nonclassic modes of action.[6−8] RAPTA-C ($[Ru^{II}(cym)(PTA)Cl_2]$, PTA = 1,3,5-triaza-7-phosphatricyclo[3.3.1.1]decane; cym = η^6-*p*-cymene) and RM175 ($[Ru^{II}(\eta^6$-biphenyl)(en)Cl$]^+$, en = ethylenediamine) are the two lead structures that have been extensively studied. Despite only small differences in their structures, these compounds exhibit contrasting biological activities and modes of action. In preclinical tests, the anticancer activity of RM175 was similar to that of cisplatin and it was more active in cisplatin-resistant *in vivo* models, while RAPTA-C emerged as an antimetastatic agent *in vivo*. Both lead compounds were extensively modified at both the arene moiety and the mono- or bidentate ligand systems to develop structure−activity relationships and to equip them with functional groups to increase their targeted properties.[9−18]

In addition to these two lead structures, several other classes of compounds based on the Ru(arene) backbone have been

Received: August 14, 2014

   dx.doi.org/10.1021/om500825h | *Organometallics* XXXX, XXX, XXX−XXX

investigated by replacing the PTA and en ligands with other mono-, bi-, and tridentate ligand systems.[3,7] It has been shown that such modification has a major impact on the anticancer activity of organoruthenium complexes. A recent trend has been to introduce chelating ligands derived from bioactive organic compounds.[3,7,19−25] Many of these examples act as *O,O*-bidentate ligand systems, forming five-membered rings with the metal center. It was shown that Ru complexes of pyrones undergo quick chlorido/aqua ligand exchange reactions, and such hydrolysis products were capable of forming adducts with DNA model compounds.[7,26−29] Coordination of the pyrone-related flavonols to Ru centers not only enhanced the bioavailability of flavonols but also provided potent multitarget antitumor agents. In addition to covalent binding to DNA, these compounds inhibit topoisomerase IIα.[20,21] Replacing pyrones with pyridone-based ligand systems resulted notably in relatively stable Ru(arene) complexes with significant cytotoxicity. In particular, dinuclear ruthenium complexes linked through pyridinone-based spacers were shown to exhibit strong anticancer properties comparable to oxaliplatin in human tumor cell lines while being able to cross-link DNA duplexes and DNA with proteins.[30,31]

These studies showed the potential of Ru(arene) complexes carrying *O,O*-bidentate ligands and prompted us to further explore this class of compounds. Turel et al. reported the Ru(arene) complexes of nalidixic acid, ofloxacin, and other antibacterial compounds.[32−34] Such ligands also feature bidentate *O,O*-donor systems forming six-membered chelates with the metal center. This is a chelation motif that may also be obtained with ligands based on the oxicam scaffold. Oxicams such as piroxicam and meloxicam (Chart 1) belong to the class

Chart 1. Structures of the Two Nonsteroidal Anti-inflammatory Drugs (NSAIDs) Piroxicam (Left) and Meloxicam (Right)

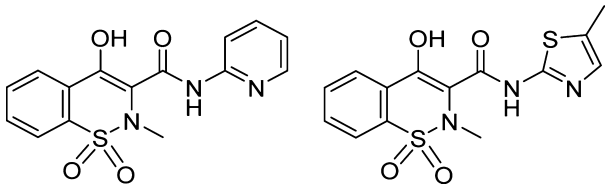

of nonsteroidal anti-inflammatory drugs (NSAIDs) and are highly efficient as treatments of rheumatologic diseases and to reduce inflammatory effects after surgery. NSAIDs exert their activity through inhibition of the cyclooxygenase (COX)-mediated production of prostaglandins (PG) or COX-independent mechanisms.[35] Cyclooxygenases (COXs) are known to play a role in tumor growth, progression, migration, and angiogenesis,[36] which makes them interesting targets to develop anticancer agents with higher selectivity than established drugs, and several oxicam derivatives were shown to inhibit cyclooxygenases.[37] In recent years several anti-inflammatory drug derivatives were coordinated to metal centers to improve their biological activity. For example, Ott et al. developed cobalt-modified acetylsalicylic acid derivatives with promising antiproliferative properties.[38,39] Copper and zinc complexes of the anti-inflammatory drug indomethacin[40] and cobalt(II) complexes with the NSAIDs mefenamic acid, tolfenamic acid, and naproxen have also been reported.[41,42] Such strategies often result in enhanced biological activity compared to the parent drugs.

Herein, we report bimodal anticancer agents based on a Ru moiety featuring a labile chlorido ligand that may allow the compound to bind covalently in a monodentate fashion to a target, such as DNA. The target molecule features on the other hand an oxicam ligand that may bind to a COX enzyme. The preparation and characterization of the complexes are complemented by cytotoxicity studies, molecular docking experiments, and binding experiments to biological molecules.

RESULTS AND DISCUSSION

The oxicam structure can be used as a scaffold to build a library of biologically active compounds. We synthesized a series of Ru(cym) complexes with *O,O*-chelating ligands derived from the oxicam backbone. The oxicam derivatives **1a−1d** were prepared by *N*-alkylation of 4-hydroxy-1,1-dioxo-1,2-dihydro-1λ^6-benzo[*e*][1,2]thiazine-3-carboxylic acid methyl ester using a previously reported procedure.[43] Ligands **1a−1d** were converted into the respective Ru(cym) complexes **2a−2d** by activating the oxicam ligands by deprotonation of the hydroxyl group at position 4. For this purpose, NaOMe was added to a stirred suspension of the ligand in dry MeOH. After stirring for about 30 min, the suspension changed in color to give a light yellow, clear solution. The Ru dimer $[Ru(cym)Cl_2]_2$ was added to this solution, and the reaction mixture was stirred for 4 h at room temperature, which resulted in precipitation of red (**2a**, **2b**) or yellow (**2c**, **2d**) solids in yields of 49−61%. When carrying out the same reaction under the same conditions but without activation of the ligands, no precipitation was observed, although the ^{1}H NMR spectra indicated incomplete complex formation. Prolonged reaction times up to 24 h did not lead to complete conversion of the starting material, and workup involving evaporation of the solvent mixture under reduced pressure followed by extraction with DCM and diethyl ether afforded the products only in very low yields (<10%).

Scheme 1. Synthetic Route to Ru^{II}(η^6-*p*-cymene) Complexes of Oxicam-Derived Ligands and NMR Numbering Scheme for Complexes 2a−2d

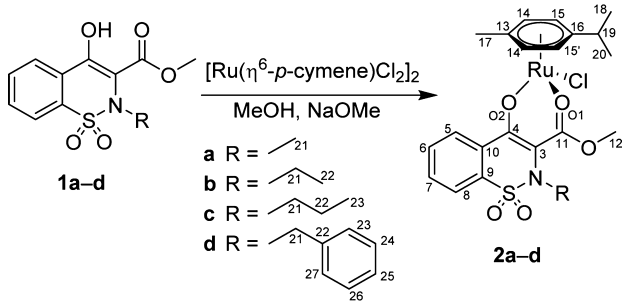

All the compounds were characterized by elemental analysis, ESI-MS, 1D and 2D NMR spectroscopy, and single-crystal X-ray diffraction analysis (**2b−2d**). Complex formation was indicated by disappearance of the O−H signal of the ligands in the ^{1}H NMR spectra at around 12 ppm and appearance of additional signals corresponding to the cym protons. An upfield shift for H^{12} (0.03−0.16 ppm) and NC−H (0.25−0.51 ppm) signals was observed upon complexation. This is probably due to the increased delocalization of electron density between two C−O groups at positions 4 and 11 of the ligand after formation of the coordination compound.

dx.doi.org/10.1021/om500825h | *Organometallics* XXXX, XXX, XXX−XXX

The formation of the complexes was also confirmed by ESI-MS. The mass spectra recorded in positive ion mode featured peaks at m/z values in close agreement with the expected values for $[M - Cl]^+$ ions, after cleavage of the labile chlorido ligand from the metal complex during the ionization process.

X-ray diffraction analyses of complexes **2b**, **2c**, and **2d** revealed a piano-stool configuration, which is characteristic of metal(arene) complexes.[7,27] The oxicam-derived ligands acted as *O,O*-chelating bidentate ligands and formed six-membered chelate rings upon binding to the Ru^{II} center (Figure 1). Notably, in the case of **2b** only a single enantiomer was identified in the molecular structure, whereas the crystal structures of **2c** and **2d** featured two chiral-at-metal center enantiomers (Figures S1 and S2). The Ru−$cym_{centroid}$ distances were 1.642, 1.653, and 1.641 Å, and the Ru—Cl bond lengths were 2.403(1), 2.420(1), and 2.396(1) Å in **2b**, **2c**, and **2d**, respectively (Tables S2 and S3). These parameters were very similar to those observed for structurally related [Ru(cym)(3-hydroxy-2-pyridone)Cl] complexes.[27]

The oxicam scaffold was nonplanar with regard to the heterocyclic ring. The nitrogen was significantly out of plane, and the torsion angles (C−C−SO_2−N) were determined as 27.40°, 31.74°, and 37.69° for **2b**, **2c**, and **2d**. This may be related to the substituents at the ring-nitrogen atom, especially with the benzyl residue tending to form π-stacking interactions with the oxicam phenyl ring and C···C distances as short as 3.321(5) Å (Figure S3). Coordination of the Ru(cym) fragment to the oxicam ligands impacted especially the C4−O2 bond lengths, which were found in **1b**−**1d**[44−46] to be 1.343(4), 1.344(2), and 1.339(17) Å. These bonds are significantly shorter in the respective complexes **2b**−**2d** (1.280(4), 1.293(3), and 1.283(4) Å, respectively), whereas the C11−O1 bond was slightly elongated due to coordination to the metal center (Tables S2 and S3). In addition, the C3−C4 distances were found to be 1.392(4), 1.389(3), and 1.397(4) Å in **2b**−**2d**, respectively, and were therefore significantly longer than in **1b**−**1d** (1.343(5), 1.346(3), and 1.369(2) Å). This indicates more single-bond character of this bond than in the free ligand, resulting in a conjugated system involving O1, C11, C3, C4, and O2.

Lipophilicity. The lipophilicity of bioactive compounds has a major impact on their accumulation in cells and especially the penetration through cell membranes. Complexes **2a**−**2d** are well soluble in apolar organic solvents such as dichloromethane and chloroform. The solubility in polar solvents especially in water is limited. Taking the solubility of the organoruthenium compounds in aqueous solutions as a measure for lipophilicity, they follow the order **2a** > **2b** > **2c** > **2d** (0.34, 0.33, 0.30, and 0.28 mM in 1% DMSO/water, respectively). This pattern may be explained by the increasing size of the substituents at the nitrogen atom in **2a** < **2b** < **2c** < **2d**. In order to quantify this observation, calculated logarithmic octanol−water partition coefficients (clog P) of **1a**−**1d** were obtained by using the software tool Molinspiration (http://www.molinspiration.com. Experimental capacity factors (log k') of **1a**−**1d** were determined by HPLC using MeOH/water mixtures containing 40−75% MeOH as eluent (Table 1). Compounds **1a**−**1d** were chosen, as the Ru(cym)Cl moiety is present in all complexes and therefore has no significant impact on the relative values. Furthermore, the complexes were found to decompose during HPLC analysis, resulting in a series of peaks including some that were assigned to an uncoordinated ligand. In order to minimize the influence of the solvent and the column conditions, the log k' values were extrapolated to 0% organic solvent, giving log k_w values.[47] Increasing the size of the *N*-

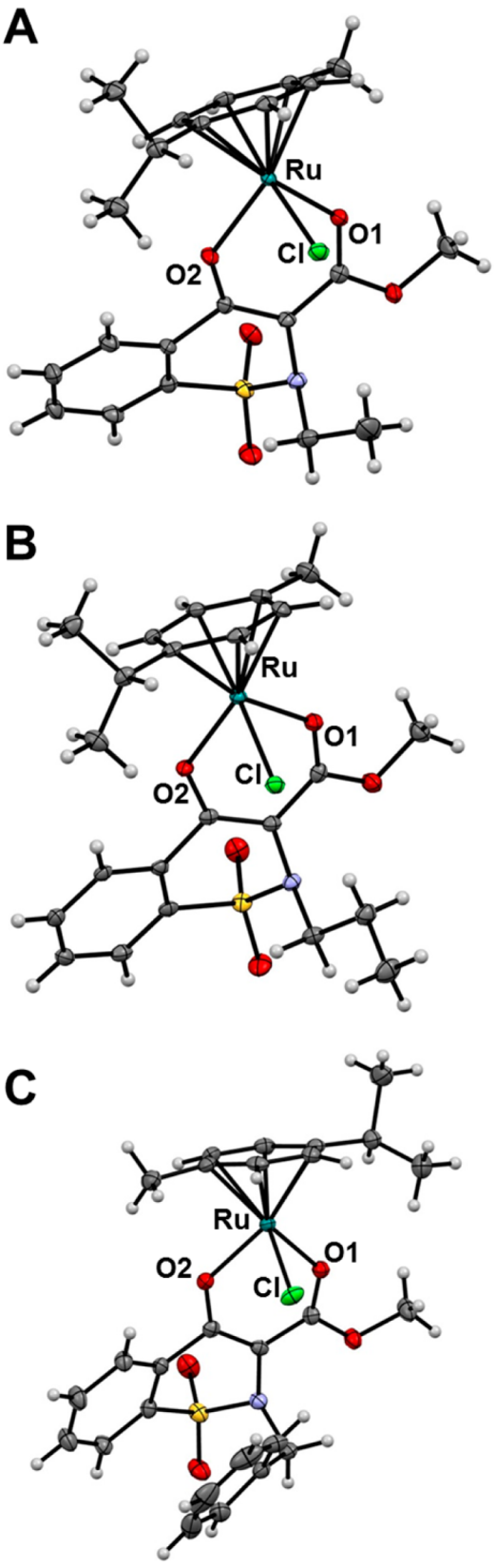

Figure 1. ORTEP diagrams of enantiomers of **2b** (A), **2c** (B), and **2d** (C) drawn at the 50% probability level. Selected bond lengths and angles around the Ru center are given in Tables S2 and S3.

dx.doi.org/10.1021/om500825h | *Organometallics* XXXX, XXX, XXX−XXX

Table 1. *In Vitro* Anticancer Activity (mean IC_{50} values ± standard deviations) of 2a−2d in Human Colon Carcinoma (HCT116) and Breast Cancer (MDA MB 231) Cell Lines (exposure time 72 h), Logarithmic Extrapolated Capacity Factors in Pure Water (log k_w),[57] and Calculated (clog *P*) Octanol−Water Partition Coefficients

	IC_{50} values/μM			
compound	HCT116	MDA MB 231	log k_w[a]	clog *P*[a]
2a	>170	>170	2.40 ± 0.02	2.0
2b	>165	>165	2.70 ± 0.05	2.4
2c	109 ± 20	>150	3.15 ± 0.06	2.9
2d	80 ± 5	>140	3.58 ± 0.07	3.4

[a]Both log k_w and clog *P* were determined for the ligands.

hydrocarbon substituent led to an increase in lipophilicity in the order **1a** < **1b** < **1c** < **1d**, with the methyl derivate **1a** being the least lipophilic (log k_w = 2.40, clog *P* = 2.0) and the benzyl derivative **1d** the most lipophilic (log k_w = 3.58, clog *P* = 3.4). Overall, the log k_w and clog *P* values for **1a**−**1d** were in good agreement with each other, as well as with the solubility data obtained for complexes **2a**−**2d**.

Stability in DMSO and Aqueous Solution. Stability in solution is an important requirement for drug candidates. DMSO is the most widely employed solvent to prepare stock solutions for biophysical and biological testing. For some transition metal complexes, DMSO acts as a good ligand, coordinating to the metal center through either the sulfur or oxygen atom.[48] Therefore, it is imperative to establish the stability of organometallic compounds in DMSO before performing biological experiments. For this purpose, **2a** and **2b** (1−2 mg) were dissolved in DMSO-d_6, and the integrity was monitored by ^{1}H NMR spectroscopy for up to 72 h. The compounds were stable in the first 3 h, and after 24 h a new species was formed as indicated by a signal at about δ = 5.8 ppm (10% relative abundance to the Ru complex), most likely due to the coordination of DMSO to the Ru center. This new signal increased further up to about 25% within 72 h for both tested compounds (Figure S4). In addition, cleavage of the cymene moiety was observed corresponding to new signals emerging at δ = 7.2 ppm after 3 h incubation time. The intensity of this signal increased significantly over 72 h, giving the major decomposition product.

For hydrolytic experiments, **2a** and **2b** were dissolved in 20% DMSO-d_6/D_2O due to insufficient solubility of the compounds in D_2O. Again a time course was recorded using ^{1}H NMR spectroscopy, and data sets were collected after 0.5, 3, 24, and 48 h (Figure 2). Both compounds hydrolyzed immediately by exchange of the chlorido ligand with a water molecule to give **2a**^{aqua} and **2b**^{aqua}. About 10% of **2a**^{aqua} and **2b**^{aqua} underwent cleavage of the oxicam ligand to form the hydroxy-bridged dimeric species $[Ru_2(\eta^6\text{-}p\text{-cymene})_2(OH)_3]^+$ after 3 h. This observation was reported for other Ru(η^6-arene) complexes with similar ligand systems.[7,27−29]

5′-GMP Binding. DNA is the primary target of the established platinum-based anticancer agents and was also suggested as a target for organoruthenium compounds. Therefore, **2a** and **2b** were incubated with the nucleotide 5′-GMP, and the reaction was monitored by ^{1}H and ^{31}P{^{1}H} NMR spectroscopy. In the ^{1}H NMR spectra we observed a slight downfield shift of the H-8 proton signal of 5′-GMP from 8.15 to 8.24 ppm. However, addition of an excess of 5′-GMP did not result in additional peaks. The ^{31}P{^{1}H} NMR spectra, however, suggested binding of the phosphate to the Ru center, as indicated by the appearance of a second signal at 3.7 ppm in addition to the peak at 2.3 ppm, assigned to 5′-GMP. This is in contrast to most other organometallic compounds, which mostly prefer to coordinate through the N7 atom rather than the phosphate. However, there have also been reports that phosphate coordination occurs initially followed by conversion to the N7 of 5′-GMP.[49]

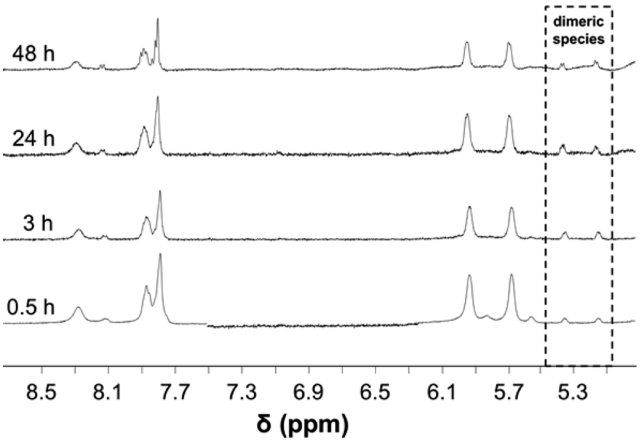

Figure 2. Stability study of **2b** in 20% DMSO-d_6/D_2O by ^{1}H NMR spectroscopy. The time-dependent spectra recorded after 0.5, 3, 24, and 48 h are shown.

Reactivity toward Amino Acids. After administration into the bloodstream, metallodrugs encounter a number of biomolecules such as proteins. Serum proteins can either act as delivery agents for anticancer metallodrugs or deactivate them before they reach their cellular target(s).[3,50−52] In order to understand reactivity and biologically relevant metabolization of organoruthenium−oxicam compounds, the reactions of **2a** and **2b** with the amino acids His, Met, and Cys were investigated by ^{1}H NMR spectroscopy. The amino acids were incubated with **2a** and **2b** in equimolar amounts in DMSO-d_6/D_2O (20%), and the reactions were monitored for 48 h. His and Met coordinate to the Ru center after release of chlorido, while the bidentate oxicam chelators still remain bound to ruthenium. In the ^{1}H NMR spectra recorded for the reaction of His with **2a**, a shift was observed for the signals assigned to the imidazole protons after coordination to the metal center (Figure 3). However, the Cys thiol exhibits a strong trans-effect and leads to decomposition of the complexes within minutes, as has been reported for related Ru(η^6-arene) complexes.[27]

***In Vitro* Anticancer Activity.** The cytotoxicity of Ru compounds **2a**−**2d** was evaluated in human colon carcinoma (HCT116) and breast cancer (MDA MB 231) cell lines by the sulforhodamine B (SRB) assay (Table 1). Compounds **2c** and **2d** exhibited modest cytotoxicity against both cancer cell lines. The lipophilicity of the complexes appears to be the determining factor for the cytotoxicity, and the most lipophilic compound, **2d**, was also the most cytotoxic, with an IC_{50} value of 80 μM against HCT116 cells. Even though the compounds were mostly noncytotoxic in both cell lines, this is not necessarily a negative property for an anticancer drug candidate. The mechanisms of action of ruthenium compounds are still not fully understood, and the examples of NAMI-A and organometallic RAPTA derivatives, which are noncytotoxic *in vitro* but exhibit high activity against metastases *in vivo*, demonstrate that IC_{50} values from medium to high μM range

dx.doi.org/10.1021/om500825h | *Organometallics* XXXX, XXX, XXX−XXX

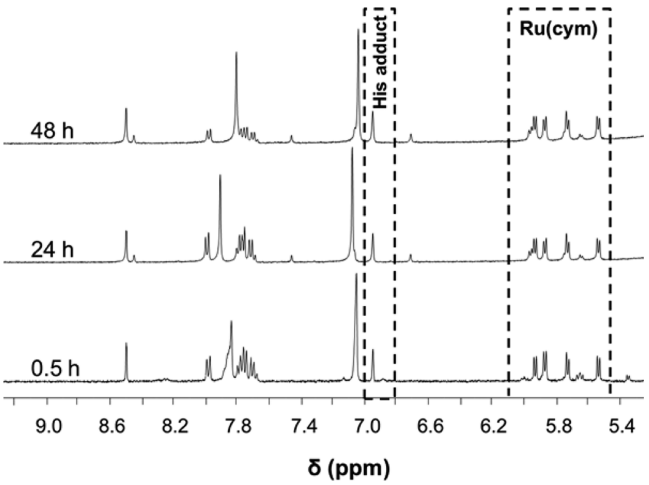

Figure 3. Reactivity of **2a** with His (1:2) in 10% DMSO-d_6/D_2O followed by ^{1}H NMR spectroscopy. The His adduct signals and the aromatic cymene protons are indicated.

are not a sufficient reason to discard a compound from further development.[53−56]

Molecular Modeling. The ligands **1a−1d** and complexes **2a−2d** were docked into the binding pocket of the COX-2 crystal structure. Reasonable scores are found for derivatives **1a−1d** for all the scoring functions akin to meloxicam, suggesting a good binding to COX-2, i.e., 51−68 for ChemPLP, 26−34 for ASP, 25−30 for CS, and finally 49−70 for the GS function (Table 4). Ligands **1a−1d** showed good overlap with GS in the binding pocket of COX-2, with the methyl derivative however slightly shifted compared to the oxicam scaffold of the other ligand structures (Figures S5 and S6). Complexes **2a−2d** could only be docked with GS, and the fitness scores predicted were substantially lower, in the range of 5−11 for **2a−2c** and with derivative **2d** giving a negative number (−26). The highest scoring configurations of ligands **1a−1d** and the respective Ru(cym) complexes showed no overlap of the oxicam backbones (see Figure 4 for **2c**).

Interestingly, **2a** and **2b**, with the smaller substituents at the heterocyclic nitrogen atom, showed good overlap, and the *n*-propyl and benzyl derivatives were well overlapped. The binding pocket of COX-2 is situated deep in the enzyme and is size-restricted. This may limit the access of larger molecules such as **2a−2d**.

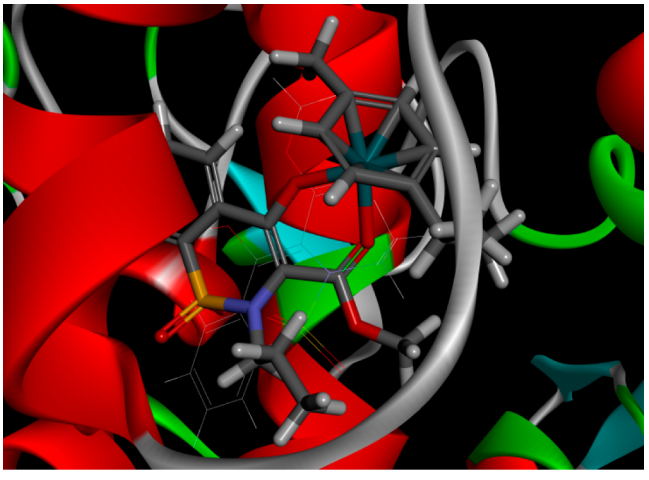

Figure 4. Overlay of the highest scoring docking configurations of **2c** in the binding site of meloxicam in COX-2.

CONCLUSIONS

In the search for new drugs, known bioactive compounds are now often repositioned and applied for the treatment of new indications. In our efforts to develop new metallodrugs, we use proven pharmacophores and coordinate them to metal fragments with established anticancer properties. In this study, we incorporated the oxicam backbone found in the nonsteroidal anti-inflammatory drugs meloxicam and piroxicam into an organometallic Ru(arene) compound. Oxicams are well-known inhibitors of cyclooxygenases, overexpressed in many tumors. In order to estimate the potential of the Ru(cym) complexes of different oxicam derivatives, their anticancer activity was studied *in vitro*, and modest cytotoxic potential was observed in HCT116 but not in MDA MB 231 cells. The most lipophilic compound, **2d**, as demonstrated by HPLC and *in silico* studies, was the most cytotoxic in the HCT116 cell line. As shown for structurally related complexes, this may be related to the properties of coordination compounds of *O,O*-chelating ligands in aqueous solution and in the presence of biomolecules. Therefore, the stability of the complexes was determined by ^{1}H NMR spectroscopy, and they were found to undergo a rapid Cl/H_2O exchange reaction in aqueous solutions. In contrast, in DMSO they were stable for up to 3 h, and only later during the course of the reaction additional species appeared featuring DMSO coordinated to the Ru center and cleavage of the *p*-cymene ligand. In addition, the reactivity toward GMP, His, Met, and Cys as biologically relevant ligands was studied. While His and Met behave as expected and replace the chlorido ligand of the complexes, Cys causes decomposition, and interestingly GMP did not bind to the metal center through its N7, but it appears as if the phosphate moiety interacted with the Ru center. Docking studies with COX-2 as the target of oxicam NSAIDs may explain the lack of anticancer activity of the compounds. While the studies with oxicam ligands **1a−1d** support binding to COX-2, the complexes gave low or negative GoldScores, suggesting targets different from those of the ligand structures.

EXPERIMENTAL SECTION

All reactions were carried out in dry solvents under an inert atmosphere unless otherwise stated. Chemicals obtained from commercial suppliers were used as received and were of analytical grade. Dichloromethane and methanol were dried using standard procedures. $RuCl_3 \cdot 3H_2O$ (40.4%) was purchased from Precious Metals Online; α-terpinene from Sigma-Aldrich; and L-histidine (His), L-methionine (Met), and L-cysteine (Cys) from AK Scientific Inc. Guanosine 5′-monophosphate disodium salt (5′-GMP) was purchased from Fluka. The dimer bis[dichlorido(η^6-*p*-cymene)ruthenium(II)][58] and the *N*-alkyl-4-hydroxy-1,1-dioxo-1,2-dihydro-1λ^6-benzo[*e*][1,2]-thiazine-3-carboxylic acid methyl ester[59] were synthesized by adapting reported procedures.

Melting points were measured using a SMP30 Stuart Scientific melting point apparatus.

Elemental analyses for all compounds were performed at the Campbell Microanalytical Laboratory, The University of Otago. High-resolution mass spectra were recorded on the Bruker microTOF-Q II electrospray ionization (ESI) mass spectrometer in positive ion mode. ^{1}H, ^{31}P{^{1}H}, and ^{13}C{^{1}H} NMR spectra were recorded on Bruker DRX 400 MHz NMR spectrometers at ambient temperature at 400.13 (^{1}H), 161.98 (^{31}P{^{1}H}), and 100.61 MHz (^{13}C{^{1}H}), and 2D NMR data were collected in a gradient-enhanced mode. ^{1}H and ^{13}C{^{1}H} chemical shifts are reported vs $SiMe_4$ and were determined by

dx.doi.org/10.1021/om500825h | *Organometallics* XXXX, XXX, XXX−XXX

reference to the residual ^{1}H and $^{13}C\{^{1}H\}$ solvent peaks. All compounds were analyzed via multinuclear 2D ($^{1}H-^{1}H$ COSY, $^{1}H-^{13}C$ HSQC, and HMBC) NMR spectroscopic experiments, allowing unambiguous assignments of characteristic resonances.

The X-ray diffraction data of crystals of **2b−2d** were collected on a Bruker Smart APEX II diffractometer with graphite-monochromatized Mo Kα radiation, λ_{Mo} = 0.710 73 Å at 100 K (see Table S1 for the measurement parameters). Data reduction was carried out using the SAINT program.[60] Semiempirical absorption corrections were applied based on equivalent reflections using SADABS.[61] The structure solution and refinements were performed with the SHELXL-2013 program package.[62]

General Procedure for Synthesis of Ru Complexes. Sodium methoxide (1.2 equiv) was added to a stirred suspension of methyl *N*-alkyl-1,1-dioxo-4-hydroxy-2*H*-1,2-benzothiazine-3-carboxylate (1.0 equiv) in dry methanol under an inert atmosphere. The dimer $[Ru(\eta^6\text{-}p\text{-cymene})Cl_2]_2$ (0.5 equiv) was added to the reaction mixture, and the reaction was further stirred at room temperature for 4 h. The reaction mixture was concentrated under reduced pressure, and the products were filtered, washed with diethyl ether (5 × 3 mL), and dried under vacuum.

Chlorido(methyl 4-oxido-2-methyl-2*H*-1,2-benzothiazine-3-carboxylate 1,1-dioxide)(η^6-*p*-cymene)ruthenium(II), 2a. The Ru(arene) complex **2a** was synthesized following the general procedure using sodium methoxide (32 mg, 0.60 mmol), methyl 4-hydroxy-2-methyl-2*H*-1,2-benzothiazine-3-carboxylate 1,1-dioxide (135 mg, 0.50 mmol), and $[Ru(\eta^6\text{-}p\text{-cymene})Cl_2]_2$ (153 mg, 0.25 mmol).

Yield: 61% (165 mg, yellow precipitate). Mp: 224−226 °C (dec). Anal. Found: C, 47.06; H, 4.53; N, 2.67; S, 5.95. Calcd for $C_{21}H_{24}ClNO_5RuS$: C, 46.79; H, 4.49; N, 2.60; S, 5.95. MS (ESI^+): m/z $[M - Cl]^+$ 504.0818. ^{1}H NMR (400.13 MHz, $CDCl_3$, 25 °C): δ 8.03 (dd, $^{3}J_{(H7,H8)}$ = 8 Hz, $^{4}J_{(H6,H8)}$ = 2 Hz, 1H, H-8), 7.66 (dd, $^{3}J_{(H5,H6)}$ = 8 Hz, $^{4}J_{(H5,H7)}$ = 2 Hz,1H, H-5), 7.57 (ddd, $^{3}J_{(H5,H6)/\ (H5,H7)}$ = 8 Hz, $^{3}J_{(H5,H6)/\ (H6,H7)}$ = 8 Hz, $^{4}J_{(H6,H8)}$ = 2 Hz, 1H, H-6), 7.52 (ddd, $^{3}J_{(H6,H7)/\ (H7,H8)}$ = 8 Hz, $^{3}J_{(H6,H7)/\ (H7,H8)}$ = 8 Hz, $^{4}J_{(H5,H7)}$ = 2 Hz, 1H, H-7), 5.30−5.45 (m, 2H, H-14/H-14′), 5.27−5.24 (m, 2H, H-15/H-15′), 3.86 (s, 3H, H-12), 2.94−2.87 (m, 1H, H-19), 2.64 (s, 3H, H-21), 2.20 (s, 3H, H-17), 1.37 (d, $^{3}J_{(H18,H19)/\ (H19,H20)}$ = 7 Hz, 3H, H-18/H-20), 1.36 (d, $^{3}J_{(H18,H19)/(H19,H20)}$ = 7 Hz, 3H, H-18/H-20). ^{13}C NMR (100.61 MHz, $CDCl_3$, 25 °C): δ 169.4 (C-11), 168.1 (C-4), 135.7 (C-9), 133.2 (C-10), 132.1 (C-8), 131.5 (C-5), 128.4 (C-6), 123.3 (C-7), 116.2 (C-3), 99.0 (C-13), 96.2 (C-16), 83.0, 82.3 (C-14/C-14′), 78.7, 79.8 (C-15/C-15′), 53.3 (C-12), 39.5 (C-21), 30.9 (C-19), 22.3, 22.4 (C-18/C-20), 17.8 (C-17).

Chlorido(methyl 4-oxido-2-ethyl-2*H*-1,2-benzothiazine-3-carboxylate 1,1-dioxide)(η^6-*p*-cymene)ruthenium(II), 2b. Complex **2b** was synthesized following the general procedure using sodium methoxide (26 mg, 0.48 mmol), methyl 4-hydroxy-2-ethyl-2*H*-1,2-benzothiazine-3-carboxylate 1,1-dioxide (113 mg, 0.40 mmol), and $[Ru(\eta^6\text{-}p\text{-cymene})Cl_2]_2$ (123 mg, 0.20 mmol).

Yield: 52% (115 mg, dark red crystals). Mp: 198−200 °C (dec). Anal. Found: C, 47.89; H, 4.96 N, 2.53; S, 5.71. Calcd for $C_{22}H_{26}ClNO_5RuS$: C, 47.78; H, 4.74; N, 2.53; S, 5.80. MS (ESI^+): m/z $[M - Cl]^+$ 518.0574. ^{1}H NMR (400.13 MHz, $CDCl_3$, 25 °C): δ 8.08 (dd, $^{3}J_{(H7,H8)}$= 8 Hz, $^{4}J_{(H6,H8)}$ = 2 Hz, 1H, H-8), 7.72 (dd, $^{3}J_{(H5,H6)}$ = 7 Hz, $^{4}J_{(H5,H7)}$ = 2 Hz, 1H, H-5), 7.61 (ddd, $^{3}J_{(H5,H6)/\ (H6,H7)}$ = 8 Hz, $^{3}J_{(H5,H6)/\ (H6,H7)}$ = 8 Hz, $^{4}J_{(H6,H8)}$ = 2 Hz, 1H, H-6), 7.57 (ddd, $^{3}J_{(H6,H7)/\ (H7,H8)}$ = 8 Hz, $^{3}J_{(H6,H7)/\ (H7,H8)}$ = 8 Hz, $^{4}J_{(H5,H7)}$ = 2 Hz, 1H, H-7), 5.62−5.58 (m, 2H, H-14/H-14′), 5.34−5.31 (m, 2H, H-15/H-15′), 3.91 (s, 3H, H-12), 3.37−3.28 (m, 1H, H-21$_\alpha$), 3.24−3.15 (m, 1H, H-21$_\beta$), 3.04−2.94 (m, 1H, H-19), 2.29 (s, 3H, H-17), 1.44 (dd, $^{3}J_{(H18,H19)/(H19,H20)}$ = 7 Hz, $^{4}J_{(H18,H20)}$ = 2 Hz, 6H, H-18/H-20), 0.72 (t, $^{3}J_{(H21,H22)}$ = 6 Hz, 3H, H-20). ^{13}C NMR (100.61 MHz, $CDCl_3$, 25 °C): δ 170.3 (C-11), 169.5(C-4), 138.4 (C-9), 133.4 (C-10), 131.8 (C-8), 131.4 (C-5), 128.4 (C-6), 122.3 (C-7), 103.0 (C-3), 98.8 (C-13), 96.1 (C-16), 82.4, 83.0 (C-14/C-14′), 78.8, 79.8 (C-15/C-15′), 53.2 (C-12), 47.6 (C-21), 35.5 (C-17), 22.3, 22.4 (C-18/C-20), 17.8 (C-19), 11.3 (C-22).

Chlorido(methyl 4-oxido-2-*n*-propyl-2*H*-1,2-benzothiazine-3-carboxylate 1,1-dioxide)(η^6-*p*-cymene)ruthenium(II), 2c. Complex **2c** was synthesized following the general procedure using sodium methoxide (26 mg, 0.48 mmol), methyl 4-hydroxy-2-*n*-propyl-2*H*-1,2-benzothiazine-3-carboxylate 1,1-dioxide (119 mg, 0.40 mmol), and $[Ru(\eta^6\text{-}p\text{-cymene})Cl_2]_2$ (123 mg, 0.20 mmol).

Yield: 56% (126 mg, dark red crystals). Mp: 192−193 °C (dec). Anal. Found: C, 49.00; H, 4.77; N, 2.55; S, 5.50. Calcd for $C_{23}H_{28}ClNO_5RuS$: C, 48.72; H, 4.98; N, 2.47; S, 5.65. MS (ESI^+): m/z $[M - Cl]^+$ 532.0718. ^{1}H NMR (400.13 MHz, $CDCl_3$, 25 °C): δ 8.08 (dd, $^{3}J_{(H7,H8)}$= 7 Hz, $^{4}J_{(H6,H8)}$ = 2 Hz, 1H, H-8), 7.71 (dd, $^{3}J_{(H5,H6)}$ = 7 Hz, $^{4}J_{(H5,H7)}$ = 2 Hz, 1H, H-5), 7.61 (ddd, $^{3}J_{(H5,H6)}$ = 8 Hz, $^{3}J_{(H6,H7)}$ = 8 Hz, $^{4}J_{(H6,H8)}$ = 2 Hz, 1H, H-6), 7.57 (ddd, $^{3}J_{(H6,H7)/\ (H7,H8)}$ = 8 Hz, $^{3}J_{(H6,H7)/\ (H7,H8)}$ = 8 Hz, $^{4}J_{(H5,H7)}$ = 1 Hz, 1H, H-7), 5.61−5.58 (m, 2H, H-14/H-14′), 5.33−5.31 (m, 2H, H-15/H-15′), 3.91 (s, 3H, H-12), 3.16−3.06 (m, 2H, H-21), 3.02−2.95 (m, 1H, H-19), 2.28 (s, 3H, H-17), 1.44 (d, $^{3}J_{(H18,H19)/(H19,H20)}$ = 7 Hz, 3H, H-18/H-20), 1.43 (d, $^{3}J_{(H18,H19)/(H19,H20)}$ = 7 Hz, 3H, H-18/H-20), 1.33−1.24 (m, 1H, H-22$_\alpha$), 1.09−0.99 (m, 1H, H-22$_\beta$), 0.59 (t, $^{3}J_{(H22,H23)}$ = 7 Hz 3H, H-23). ^{13}C NMR (100.61 MHz, $CDCl_3$, 25 °C): δ 170.1(C-11), 169.5 (C-4), 138.1 (C-9), 133.2 (C-10), 131.8 (C-8), 131.4 (C-5), 128.4 (C-6), 122.4 (C-7), 103.8 (C-3), 98.9 (C-13), 96.1 (C-16), 83.0, 82.4 (C-14/C-14′), 79.8, 78.8 (C-15/C-15′), 54.6 (C-12), 53.2 (C-21), 30.9 (C-19), 22.3, 22.4 (C-18/C-20), 19.4 (C-22), 17.8 (C-17), 10.9 (C-23).

Chlorido(methyl 4-oxido-2-benzyl-2*H*-1,2-benzothiazine-3-carboxylate 1,1-dioxide)(η^6-*p*-cymene)ruthenium(II), 2d. Complex **2d** was synthesized following the general procedure using sodium methoxide (26 mg, 0.48 mmol), methyl 4-hydroxy-2-benzyl-2*H*-1,2-benzothiazine-3-carboxylate 1,1-dioxide (138 mg, 0.40 mmol), and $[Ru(\eta^6\text{-}p\text{-cymene})Cl_2]_2$ (123 mg, 0.20 mmol).

Yield: 49% (120 mg, orange crystals). Mp: 233−234 °C (dec). Anal. Found: C, 52.80; H, 4.72 N, 2.31; S, 5.25. Calcd for $C_{28}H_{31}ClNO_5RuS$: C, 52.72; H, 4.59; N, 2.28; S, 5.21. MS (ESI^+): m/z $[M - Cl]^+$ 580.0727. ^{1}H NMR (400.13 MHz, $CDCl_3$, 25 °C): δ 7.71−7.68 (m, 1H, H-8), 7.55−7.53 (m, 1H, H-5), 7.39−7.36 (m, 2H, H-6/H-7), 7.11−7.09 (m, 2H, H-24/H-26), 6.92−6.90 (m, 3H, H-23, H-25, H-27), 5.60 (d, $^{3}J_{(H14,H15)/(H14',H15')}$ = 6 Hz, 1H, H-14/H-14′), 5.56 (d, $^{3}J_{(H14,H15)/(H14',H15')}$ = 6 Hz, 1H, H-14/H-14′), 5.31−5.29 (m, 2H, H-15, H-15′), 4.42 (d, $^{2}J_{(H21\alpha,H21\beta)}$ = 14 Hz, 1H, H-21$_\beta$), 4.15 (d, $^{2}J_{(H21\alpha,H21\beta)}$ = 14 Hz, H-21$_\alpha$), 3.79 (s, 3H, H-12), 2.98−2.91 (m, 1H, H-19), 1.43 (d, $^{3}J_{(H18,H19)/(H19,H20)}$ = 7 Hz, 3H, H-18/H-20), 1.42 (d, $^{3}J_{(H18,H19)/(H19,H20)}$ = 7 Hz, 3H, H-18/H-20). ^{13}C NMR (100.61 MHz, $CDCl_3$, 25 °C): δ 170.8 (C-11), 169.6 (C-4), 138.1 (C-9), 133.4 (C-10), 132.6 (C-22), 131.4 (C-8), 130.7 (C-5), 130.5 (C-24/C-26), 127.7 (C-6), 127.4 (C-23/C-27), 127.3 (C-25), 122.23 (C-7), 98.9 (C-3), 98.5 (C-13), 96.3 (C-16), 83.1, 82.4 (C-14/C-14′), 79.8, 78.6 (C-15/C-15′), 56.4 (C-12), 53.1 (C-21), 30.9 (C-19), 22.2, 22.4 (C-18/C-20), 17.8 (C-17).

Stability Studies in DMSO and Aqueous Solution. For stability in DMSO, **2a** and **2b** (1−2 mg/mL) were dissolved in DMSO-d_6, and ^{1}H NMR spectra were recorded after 0.5, 3, 24, 48, and 72 h. Hydrolytic stability test was carried out by dissolving **2a** and **2b** (1−2 mg/mL) in DMSO-d_6/D_2O (20/80), and ^{1}H NMR was measured after 0.5, 3, 24, and 48 h.

Reactivity with Small Biomolecules. In order to investigate the reactivity of complexes with amino acids, a solution of **2a** and **2b** (1 mg/mL) in DMSO-d_6/D_2O (20/80) was treated with equimolar amounts of Cys, His, and Met, and the ^{1}H NMR spectra were recorded after 30 min, 24 h, and 48 h. For the 5′-GMP binding experiment, **2a** and **2b** were first dissolved in DMSO-d_6/D_2O (20/80); then 2 equiv of 5′-GMP was added to each of the above solutions and the reaction was monitored by ^{1}H and $^{31}P\{^{1}H\}$ NMR spectroscopy.

Determination of clog *P* and log k_w Values. Calculated logarithms of octanol−water partition coefficient (clog *P*) were obtained by using Molinspiration found at http://www.molinspiration.com.

Experimental logarithmic capacity factors (log k' values) were determined according to the OECD Guidelines for HPLC.[57] A ThermoFisher Dionex UltiMate3000 HPLC system controlled via the

Chromeleon 7.1.2 software suite (ThermoFisher Dionex) and equipped with a diode array UV−vis detector (DAD-3000 RS, ThermoFisher Dionex) was used for the measurements. The column compartment was thermostated at 25 °C, and a C_{18} reverse-phase column (Hypersil Gold, 250 mm length, 4.6 mm inner diameter, pore size 5 μm, ThermoFisher) was used as stationary phase. Thiourea (100 μM) was added as an internal standard to determine the column dead-time, and 10 μL of 100 μM samples dissolved in 1:1 MeOH/H_2O was injected. Isocratic runs using methanol/water mixtures with at least five different methanol contents between 40% and 75% were used in order to delineate the lipophilicity, and peaks were detected at 220 nm. Log k_w' values were determined by linear regression of the equation $\log k' = S \times \varphi + \log k_w$, where $k' = (t_R - t_0)/t_0$ (t_R equals the retention time on the column and t_0 is the column dead-time, i.e., the retention time of thiourea), S is the slope, φ is the organic solvent ratio, and log k_w is the logarithmic capacity factor extrapolated for pure water, i.e., $\varphi = 0$.[47] Log k' values were only considered if $-0.5 < \log k' < 1.5$ in order to ensure that the above-mentioned relationship was indeed in the linear range.[47] Measurements for all compounds were done in triplicate, and the numbers given are mean ± standard deviation.

Sulforhodamine B Assay. HCT116 and MDA MB 231 cells were supplied by ATCC and Dr. Adam Patterson, University of Manchester, UK, respectively, and were grown in αMEM (Life Technologies) supplemented with 5% fetal calf serum (Moregate Biotech). Cells were seeded at 750 (HCT116) or 10 000 (MDA MB 231) cells/well in 96-well plates and left to settle for 24 h at 37 °C and 5% CO_2. Compounds were added to the plates in a series of 3-fold dilutions in 0.5% DMSO or less for 72 h before the assay was terminated by addition of 10% trichloroacetic acid (Merck Millipore) at 4 °C for 1 h. Cells were stained with 0.4% sulforhodamine B (Sigma-Aldrich) in 1% acetic acid for 30 min in the dark at room temperature, then washed in 1% acetic acid to remove unbound dye. The stain was solubilized in unbuffered Tris base (10 mM; Serva) for 30 min on a plate shaker in the dark and quantitated on a BioTek EL808 microplate reader at an absorbance of 490 nm with a reference wavelength of 450 nm. The 10-point IC_{50} values were calculated by fitting the inhibition data relative to no inhibitor controls and proliferation at the time of compound addition to a four-parameter logistic sigmoidal dose−response curve using Prism 6.03 (GraphPad).

Molecular Modeling. The compounds were docked to the crystal structure of COX-2 (PDB ID: 4M11, resolution 2.45 Å),[63] which was obtained from the Protein Data Bank (PDB).[64,65] Scigress Ultra 7.7.0.47[66] was used to prepare the crystal structure for docking; that is, hydrogen atoms were added, and the cocrystallized meloxicam was removed as well as crystallographic water molecules. The Scigress software suite was also used to build the inhibitors, and the MM2[67] force field was used to optimize the structures. The center of the binding pocket was defined as the position of the hydroxyl oxygen atom in meloxicam (x = 67.830, y = 15.016, z = 24.355) with 10 Å radius. Fifty docking runs were allowed for each ligand with default search efficiency (100%). The basic amino acids lysine and arginine were defined as protonated. Furthermore, aspartic and glutamic acids were assumed to be deprotonated. The GoldScore (GS),[68] ChemScore (CS),[69,70] ChemPLP,[71] and ASP[72] scoring functions were implemented to validate the predicted binding modes and relative energies of the ligands using the GOLD v5.2 software suite. Meloxicam was redocked into the binding pocket using the four scoring functions and correlated to the cocrystallized conformation. The root-mean-square deviation between the heavy atoms of the cocrystallized ligand and its docked counterparts was as follows: ChemPLP 0.31 Å, ASP 0.49 Å, CS 2.10 Å, and GS 1.56 Å.

■ ASSOCIATED CONTENT

Supporting Information

The Supporting Information includes additional X-ray crystallographic and molecular modeling data. This material is available free of charge via the Internet at http://pubs.acs.org. The crystallographic data are also available from the Cambridge Crystallographic Data Centre as supplementary publication nos. CCDC 1015715−1015717 (www.ccdc.cam.ac.uk/data_request/cif).

■ AUTHOR INFORMATION

Corresponding Authors

*(W. A. Siddiqui) E-mail: waseeq786@gmail.com. Tel: +92-48-9230811-15, ext 350. Fax: +92-48-3222121.

*(C. G. Hartinger) E-mail: c.hartinger@auckland.ac.nz. Tel: +64-9-3737 599, ext 83220. Fax: +64-9-3737 599, ext 87422.

Notes

The authors declare no competing financial interests.

■ ACKNOWLEDGMENTS

We thank the University of Auckland, the Higher Education Commission of Pakistan (research project NRPU 20-1582 and IRSIP to F.A.), Genesis Oncology Trust (GOT-1263-RPG), IRSIP (F.A.), the Austrian Science Fund (Schrödinger fellowship to M.H.), and COST CM1105 for financial support. The authors are grateful to Tanya Groutso for collecting the X-ray crystal data, Nick Lloyd for ESI-MS analyses, and Emma Richardson for *in vitro* anticancer activity testing. This article is dedicated to Prof. Gerard Jaouen on the occasion of his 70th birthday.

■ REFERENCES

(1) Barry, N. P. E.; Sadler, P. J. *Chem. Commun.* **2013**, *49*, 5106−5131.
(2) Kelland, L. *Nat. Rev. Cancer* **2007**, *7*, 573−584.
(3) Hartinger, C. G.; Metzler-Nolte, N.; Dyson, P. J. *Organometallics* **2012**, *31*, 5677−5685.
(4) Hartinger, C. G.; Jakupec, M. A.; Zorbas-Seifried, S.; Groessl, M.; Egger, A.; Berger, W.; Zorbas, H.; Dyson, P. J.; Keppler, B. K. *Chem. Biodiversity* **2008**, *5*, 2140−2155.
(5) Hartinger, C. G.; Zorbas-Seifried, S.; Jakupec, M. A.; Kynast, B.; Zorbas, H.; Keppler, B. K. *J. Inorg. Biochem.* **2006**, *100*, 891−904.
(6) Meier, S. M.; Hanif, M.; Adhireksan, Z.; Pichler, V.; Novak, M.; Jirkovsky, E.; Jakupec, M. A.; Arion, V. B.; Davey, C. A.; Keppler, B. K.; Hartinger, C. G. *Chem. Sci.* **2013**, *4*, 1837−1846.
(7) Kandioller, W.; Kurzwernhart, A.; Hanif, M.; Meier, S. M.; Henke, H.; Keppler, B. K.; Hartinger, C. G. *J. Organomet. Chem.* **2011**, *696*, 999−1010.
(8) Hanif, M.; Schaaf, P.; Kandioller, W.; Hejl, M.; Jakupec, M. A.; Roller, A.; Keppler, B. K.; Hartinger, C. G. *Aust. J. Chem.* **2010**, *63*, 1521−1528.
(9) Berger, I.; Hanif, M.; Nazarov, A. A.; Hartinger, C. G.; John, R. O.; Kuznetsov, M. L.; Groessl, M.; Schmitt, F.; Zava, O.; Biba, F.; Arion, V. B.; Galanski, M.; Jakupec, M. A.; Juillerat-Jeanneret, L.; Dyson, P. J.; Keppler, B. K. *Chem.—Eur. J.* **2008**, *14*, 9046−9057.
(10) Hanif, M.; Meier, S. M.; Kandioller, W.; Bytzek, A.; Hejl, M.; Hartinger, C. G.; Nazarov, A. A.; Arion, V. B.; Jakupec, M. A.; Dyson, P. J.; Keppler, B. K. *J. Inorg. Biochem.* **2011**, *105*, 224−231.
(11) Hanif, M.; Nazarov, A. A.; Legin, A.; Groessl, M.; Arion, V. B.; Jakupec, M. A.; Tsybin, Y. O.; Dyson, P. J.; Keppler, B. K.; Hartinger, C. G. *Chem. Commun.* **2012**, *48*, 1475−1477.
(12) Nowak-Sliwinska, P.; van Beijnum, J. R.; Casini, A.; Nazarov, A. A.; Wagnieres, G.; van den Bergh, H.; Dyson, P. J.; Griffioen, A. W. *J. Med. Chem.* **2011**, *54*, 3895−3902.
(13) Tan, Y. Q.; Dyson, P. J.; Ang, W. H. *Organometallics* **2011**, *30*, 5965−5971.
(14) Kilpin, K. J.; Clavel, C. M.; Edafe, F.; Dyson, P. J. *Organometallics* **2012**, *31*, 7031−7039.
(15) Noffke, A. L.; Habtemariam, A.; Pizarro, A. M.; Sadler, P. J. *Chem. Commun. (Cambridge, U. K.)* **2012**, *48*, 5219−5246.
(16) Hu, W.; Luo, Q.; Ma, X.; Wu, K.; Liu, J.; Chen, Y.; Xiong, S.; Wang, J.; Sadler, P. J.; Wang, F. *Chem.—Eur. J.* **2009**, *15* (6586−6594), S6586/1−S6586/3.

(17) Habtemariam, A.; Melchart, M.; Fernandez, R.; Parsons, S.; Oswald, I. D. H.; Parkin, A.; Fabbiani, F. P. A.; Davidson, J. E.; Dawson, A.; Aird, R. E.; Jodrell, D. I.; Sadler, P. J. *J. Med. Chem.* **2006**, *49*, 6858−6868.
(18) Bugarcic, T.; Habtemariam, A.; Deeth, R. J.; Fabbiani, F. P. A.; Parsons, S.; Sadler, P. J. *Inorg. Chem.* **2009**, *48*, 9444−9453.
(19) Kljun, J.; Bytzek, A. K.; Kandioller, W.; Bartel, C.; Jakupec, M. A.; Hartinger, C. G.; Keppler, B. K.; Turel, I. *Organometallics* **2011**, *30*, 2506−2512.
(20) Kurzwernhart, A.; Kandioller, W.; Bartel, C.; Bachler, S.; Trondl, R.; Muhlgassner, G.; Jakupec, M. A.; Arion, V. B.; Marko, D.; Keppler, B. K.; Hartinger, C. G. *Chem. Commun.* **2012**, *48*, 4839−4841.
(21) Kurzwernhart, A.; Kandioller, W.; Bachler, S.; Bartel, C.; Martic, S.; Buczkowska, M.; Muhlgassner, G.; Jakupec, M. A.; Kraatz, H. B.; Bednarski, P. J.; Arion, V. B.; Marko, D.; Keppler, B. K.; Hartinger, C. G. *J. Med. Chem.* **2012**, *55*, 10512−10522.
(22) Meier, S. M.; Hanif, M.; Adhireksan, Z.; Pichler, V.; Novak, M.; Jirkovsky, E.; Jakupec, M. A.; Arion, V. B.; Davey, C. A.; Keppler, B. K.; Hartinger, C. G. *Chem. Sci.* **2013**, *4*, 1837−1846.
(23) Kandioller, W.; Balsano, E.; Meier, S. M.; Jungwirth, U.; Goeschl, S.; Roller, A.; Jakupec, M. A.; Berger, W.; Keppler, B. K.; Hartinger, C. G. *Chem. Commun. (Cambridge, U. K.)* **2013**, *49*, 3348−3350.
(24) Dobrov, A.; Goeschl, S.; Jakupec, M. A.; Popovic-Bijelic, A.; Graeslund, A.; Rapta, P.; Arion, V. B. *Chem. Commun. (Cambridge, U. K.)* **2013**, *49*, 10007−10009.
(25) Filak, L. K.; Goeschl, S.; Heffeter, P.; Ghannadzadeh Samper, K.; Egger, A. E.; Jakupec, M. A.; Keppler, B. K.; Berger, W.; Arion, V. B. *Organometallics* **2013**, *32*, 903−914.
(26) Henke, H.; Kandioller, W.; Hanif, M.; Keppler, B. K.; Hartinger, C. G. *Chem. Biodiversity* **2012**, *9*, 1718−1727.
(27) Hanif, M.; Henke, H.; Meier, S. M.; Martic, S.; Labib, M.; Kandioller, W.; Jakupec, M. A.; Arion, V. B.; Kraatz, H. B.; Keppler, B. K.; Hartinger, C. G. *Inorg. Chem.* **2010**, *49*, 7953−7963.
(28) Enyedy, E. A.; Bognar, G. M.; Kiss, T.; Hanif, M.; Hartinger, C. G. *J. Organomet. Chem.* **2013**, *734*, 38−44.
(29) Enyedy, E. A.; Sija, E.; Jakusch, T.; Hartinger, C. G.; Kandioller, W.; Keppler, B. K.; Kiss, T. *J. Inorg. Biochem.* **2013**, *127*, 161−168.
(30) Mendoza-Ferri, M. G.; Hartinger, C. G.; Nazarov, A. A.; Eichinger, R. E.; Jakupec, M. A.; Severin, K.; Keppler, B. K. *Organometallics* **2009**, *28*, 6260−6265.
(31) Mendoza-Ferri, M. G.; Hartinger, C. G.; Mendoza, M. A.; Groessl, M.; Egger, A. E.; Eichinger, R. E.; Mangrum, J. B.; Farrell, N. P.; Maruszak, M.; Bednarski, P. J.; Klein, F.; Jakupec, M. A.; Nazarov, A. A.; Severin, K.; Keppler, B. K. *J. Med. Chem.* **2009**, *52*, 916−925.
(32) Hudej, R.; Kljun, J.; Kandioller, W.; Repnik, U.; Turk, B.; Hartinger, C. G.; Keppler, B. K.; Miklavčič, D.; Turel, I. *Organometallics* **2012**, *31*, 5867−5874.
(33) Turel, I.; Kljun, J.; Perdih, F.; Morozova, E.; Bakulev, V.; Kasyanenko, N.; Byl, J. A. W.; Osheroff, N. *Inorg. Chem.* **2010**, *49*, 10750−10752.
(34) Kljun, J.; Bytzek, A. K.; Kandioller, W.; Bartel, C.; Jakupec, M. A.; Hartinger, C. G.; Keppler, B. K.; Turel, I. *Organometallics* **2011**, *30*, 2506−2512.
(35) Vane, S. J. *J. Clin. Rheumatol.* **1998**, *4*, S3−10.
(36) Zha, S.; Yegnasubramanian, V.; Nelson, W. G.; Isaacs, W. B.; De Marzo, A. M. *Cancer Lett.* **2004**, *215*, 1−20.
(37) Smith, H. S.; Baird, W. *Am. J. Hospice Palliative Care* **2003**, *20*, 297−306.
(38) Ott, I.; Schmidt, K.; Kircher, B.; Schumacher, P.; Wiglenda, T.; Gust, R. *J. Med. Chem.* **2005**, *48*, 622−629.
(39) Ott, I.; Kircher, B.; Bagowski, C. P.; Vlecken, D. H. W.; Ott, E. B.; Will, J.; Bensdorf, K.; Sheldrick, W. S.; Gust, R. *Angew. Chem., Int. Ed.* **2009**, *48*, 1160−1163.
(40) Dillon, C. T.; Hambley, T. W.; Kennedy, B. J.; Lay, P. A.; Zhou, Q.; Davies, N. M.; Biffin, J. R.; Regtop, H. L. *Chem. Res. Toxicol.* **2003**, *16*, 28−37.
(41) Dimiza, F.; Papadopoulos, A. N.; Tangoulis, V.; Psycharis, V.; Raptopoulou, C. P.; Kessissoglou, D. P.; Psomas, G. *Dalton Trans.* **2010**, *39*, 4517−4528.
(42) Psomas, G.; Kessissoglou, D. P. *Dalton Trans.* **2013**, *42*, 6252−6276.
(43) Siddiqui, W. A.; Ahmad, S.; Khan, I. U.; Siddiqui, H. L.; Weaver, G. W. *Synth. Commun.* **2007**, *37*, 767−773.
(44) Arshad, M. N.; Zia-Ur-Rehman, M.; Khan, I. U. *Acta Crystallogr. Sect. E Struct. Rep. Online* **2009**, *65*, o3025.
(45) Arshad, M. N.; Zia-Ur-Rehman, M.; Khan, I. U. *Acta Crystallogr. Sect. E Struct. Rep. Online* **2010**, *66*, o1070.
(46) Arshad, M. N.; Khan, I. U.; Zia-Ur-Rehman, M.; Shafiq, M.; Asiri, A. M. *Acta Crystallogr. Sect. E Struct. Rep. Online* **2011**, *67*, o1588−9.
(47) Valkó, K. *J. Chromatogr. A* **2004**, *1037*, 299−310.
(48) Patra, M.; Joshi, T.; Pierroz, V.; Ingram, K.; Kaiser, M.; Ferrari, S.; Spingler, B.; Keiser, J.; Gasser, G. *Chem.—Eur. J.* **2013**, *19*, 14768−14772.
(49) Chen, H.; Parkinson, J. A.; Morris, R. E.; Sadler, P. J. *J. Am. Chem. Soc.* **2002**, *125*, 173−186.
(50) Meier, S. M.; Babak, M. V.; Keppler, B. K.; Hartinger, C. G. *ChemMedChem* **2014**, DOI: 10.1002/cmdc.201400020.
(51) Meier, S. M.; Hanif, M.; Kandioller, W.; Keppler, B. K.; Hartinger, C. G. *J. Inorg. Biochem.* **2012**, *108*, 91−95.
(52) Novakova, O.; Nazarov, A. A.; Hartinger, C. G.; Keppler, B. K.; Brabec, V. *Biochem. Pharmacol.* **2009**, *77*, 364−374.
(53) Sava, G.; Capozzi, I.; Clerici, K.; Gagliardi, G.; Alessio, E.; Mestroni, G. *Clin. Exp. Metastasis* **1998**, *16*, 371−379.
(54) Sava, G.; Gagliardi, R.; Cocchietto, M.; Clerici, K.; Capozzi, I.; Marrella, M.; Alessio, E.; Mestroni, G.; Milanino, R. *Pathol. Oncol. Res.* **1998**, *4*, 30−36.
(55) Rademaker-Lakhai, J. M.; Van Den Bongard, D.; Pluim, D.; Beijnen, J. H.; Schellens, J. H. M. *Clin. Cancer Res.* **2004**, *10*, 3717−3727.
(56) Scolaro, C.; Bergamo, A.; Brescacin, L.; Delfino, R.; Cocchietto, M.; Laurenczy, G.; Geldbach, T. J.; Sava, G.; Dyson, P. J. *J. Med. Chem.* **2005**, *48*, 4161−4171.
(57) OECD. *OECD Guidelines for the Testing of Chemicals Test No. 117: Partition Coefficient (n-octanol/water), HPLC Method*; 2004.
(58) Bennett, M. A.; Smith, A. K. *J. Chem. Soc., Dalton Trans.* **1974**, 233−241.
(59) Ahmad, N.; Zia-ur-Rehman, M.; Siddiqui, H. L.; Ullah, M. F.; Parvez, M. *Eur. J. Med. Chem.* **2011**, *46*, 2368−2377.
(60) *SAINT, Area Detector Integration Software*; Siemens Analytical Instruments Inc.: Madison, WI, USA, 1995.
(61) Sheldrick, G. M. *SADABS, Program for Semi-empirical Absorption Correction*; University of Göttingen: Göttingen, Germany, 1997.
(62) Sheldrick, G. M. *Acta Crystallogr., Sect. A: Found. Crystallogr.* **2008**, *A64*, 112−122.
(63) Xu, S.; Hermanson, D. J.; Banerjee, S.; Ghebreselasie, K.; Clayton, G. M.; Garavito, R. M.; Marnett, L. J. *J. Biol. Chem.* **2014**, *289*, 6799−6808.
(64) Berman, H. M.; Westbrook, J.; Feng, Z.; Gilliland, G.; Bhat, T. N.; Weissig, H.; Shindyalov, I. N.; Bourne, P. E. *Nucleic Acids Res.* **2000**, *28*, 235−242.
(65) Berman, H.; Henrick, K.; Nakamura, H. *Nat. Struct. Biol.* **2003**, *10*, 980.
(66) *Scigress Explorer Ultra* Version 7.7.0.47; Fijitsu Limited, 2000−2007.
(67) Allinger, N. L. *J. Am. Chem. Soc.* **1977**, *99*, 8127−8134.
(68) Jones, G.; Willet, P.; Glen, R. C.; Leach, A. R.; Taylor, R. *J. Mol. Biol.* **1997**, *267*, 727−748.
(69) Eldridge, M. D.; Murray, C.; Auton, T. R.; Paolini, G. V.; Mee, P. M. *J. Comput.-Aided Mol. Des.* **1997**, *11*, 425−445.
(70) Verdonk, M. L.; Cole, J. C.; Hartshorn, M. J.; Murray, C. W.; Taylor, R. D. *Proteins* **2003**, *52*, 609−623.
(71) Korb, O.; Stützle, T.; Exner, T. E. *J. Chem. Inf. Model.* 2009, *49*, 84−96.
(72) Mooij, W. T. M.; Verdonk, M. L. *Proteins* **2005**, *61*, 272−287.